

# Probing the scalar-pseudoscalar mixing in the 125 GeV Higgs particle with current data

A. Barroso,<sup>1</sup> P. M. Ferreira,<sup>2,1,\*</sup> Rui Santos,<sup>2,1,†</sup> and João P. Silva<sup>2,3,‡</sup>

<sup>1</sup>*Centro de Física Teórica e Computacional, Faculdade de Ciências,  
Universidade de Lisboa, Av. Prof. Gama Pinto 2, 1649-003 Lisboa, Portugal*

<sup>2</sup>*Instituto Superior de Engenharia de Lisboa, 1959-007 Lisboa, Portugal*

<sup>3</sup>*Centro de Física Teórica de Partículas (CFTP), Instituto Superior Técnico,  
Universidade Técnica de Lisboa, 1049-001 Lisboa, Portugal*

(Dated: November 23, 2018)

LHC has found hints for a Higgs particle of 125 GeV. We investigate the possibility that such a particle is a mixture of scalar and pseudoscalar states. For definiteness, we concentrate on a two Higgs doublet model with explicit CP violation and soft  $Z_2$  violation. Including all Higgs production mechanisms, we determine the current constraints obtained by comparing  $h \rightarrow \gamma\gamma$  with  $h \rightarrow VV^*$ , and comment on the information which can be gained by measurements of  $h \rightarrow b\bar{b}$ . We find bounds  $|s_2| \lesssim 0.83$  at one sigma, where  $|s_2| = 0$  ( $|s_2| = 1$ ) corresponds to a pure scalar (pure pseudoscalar) state.

PACS numbers: 12.60.Fr, 14.80.Ec, 14.80.-j

## I. INTRODUCTION

Recently, ATLAS [1] and CMS [2] have reported tantalizing signals for a 125 GeV Higgs particle. The exact properties of this particle will be probed in the coming years. In particular, it could be a mixture of scalar and pseudoscalar states. Some authors have already studied the possibility that the 125 GeV particle is a pure pseudoscalar state, both within the two Higgs doublet model (2HDM) [3, 4] and in a more general context [5]. However, as the authors point out, this possibility is at odds with the current  $h \rightarrow VV^*$  signal, since a pure pseudoscalar state does not couple to  $VV$  (where  $V = Z, W$ ). Thus, the bounds on  $h \rightarrow VV^*$  should allow us to constrain the amount of the pseudoscalar component in the 125 GeV Higgs. In this article, we study this issue in the context of a 2HDM [6] with explicit CP violation and soft-breaking of the usual  $Z_2$  symmetry. This model has been advocated in Refs. [7–14].

We concentrate on models of type I, where all fermions couple to the same Higgs field, and models of type II, where the up type quarks couple to one Higgs field, while the down type quarks and the charged leptons couple to the other. The constraints placed by current data on the type I and type II CP conserving models (as well as on the lepton-specific and flipped models), have already been studied in Ref. [15], assuming that the 125 GeV particle is the lightest scalar, in Ref. [16], under the hypothesis that the 125 GeV particle is the heaviest scalar, and in Ref. [3], assuming a pure pseudoscalar. These studies assume Higgs production exclusively through gluon-gluon fusion and assume that the remaining scalar particles have very large masses. In our study of scalar-pseudoscalar mixing, we remove these restrictions, considering also inclusive production through vector boson fusion, associated production of a scalar and a vector boson and  $b\bar{b} \rightarrow H$  production. We also improve on Refs. [3, 15, 16] by allowing any scalar masses and mixings consistent with experiment and with the theoretical constraints from positivity, unitarity, perturbativity, and the oblique radiative corrections.

In section II we describe succinctly the 2HDM with explicit CP violation and soft  $Z_2$  violation which we will use as a concrete example of scalar-pseudoscalar mixing, relegating to appendix A the formulae we have used. In section III we show our main results, and we conclude in section IV.

---

\*E-mail: ferreira@cii.fc.ul.pt

†E-mail: rsantos@cii.fc.ul.pt

‡E-mail: jpsilva@cftp.ist.utl.pt

## II. A SPECIFIC MODEL FOR SCALAR-PSEUDOSCALAR MIXING

As a specific example of scalar-pseudoscalar mixing, we will study a model with two Higgs doublets  $(\phi_1, \phi_2)$ , with explicit CP violation, and with soft-violation of the  $Z_2$  symmetry  $\phi_1 \rightarrow \phi_1, \phi_2 \rightarrow -\phi_2$ . As far as we know, this model was first written by Ginzburg, Krawczyk and Osland [7]. It was later studied in detail in Refs. [7–13]. Here, we will follow the notation of Arhrib *et. al* [14], which has a very clear presentation of this model. For ease of reference, we collect here some of its most important characteristics.

The Higgs potential of this model is

$$\begin{aligned} V_H = & -\frac{m_{11}^2}{2}|\phi_1|^2 - \frac{m_{22}^2}{2}|\phi_2|^2 - \frac{m_{12}^2}{2}\phi_1^\dagger\phi_2 - \frac{(m_{12}^2)^*}{2}\phi_2^\dagger\phi_1 \\ & + \frac{\lambda_1}{2}|\phi_1|^4 + \frac{\lambda_2}{2}|\phi_2|^4 + \lambda_3|\phi_1|^2|\phi_2|^2 + \lambda_4(\phi_1^\dagger\phi_2)(\phi_2^\dagger\phi_1) \\ & + \frac{\lambda_5}{2}(\phi_1^\dagger\phi_2)^2 + \frac{\lambda_5^*}{2}(\phi_2^\dagger\phi_1)^2, \end{aligned} \quad (1)$$

where hermiticity forces all couplings to be real, except  $m_{12}^2$  and  $\lambda_5$ . If the latter are complex and  $\arg(\lambda_5) \neq 2\arg(m_{12}^2)$ , then there is explicit CP violation in the Higgs potential. In addition, we also allow for explicit CP violation in the Yukawa terms, leading to CP violation through the CKM matrix, as is needed to account for the current data on CP violation in the  $K$  and  $B$  systems. The  $m_{12}^2$  terms constitute a soft violation of the  $Z_2$  symmetry, which does not affect the renormalizability of the theory (the renormalization group equations of the quartic terms do not depend on the quadratic terms). Naturally, one can change the phases of the  $\phi_1$  and  $\phi_2$  fields; any physical observable must be rephasing invariant [17]. An overall phase corresponds to a global hypercharge transformation, and has no effect on the lagrangian; it can be used to render the vacuum expectation value (vev) of  $\phi_1$  real. Rephasing  $\phi_2$  can now be used to render its vev also real,

$$\langle\phi_1\rangle = v_1/\sqrt{2}, \quad \langle\phi_2\rangle = v_2/\sqrt{2}, \quad (2)$$

substantially simplifying the minimization conditions, which become

$$\begin{aligned} m_{11}^2 &= -\text{Re}(m_{12}^2) \frac{v_2}{v_1} + \lambda_1 v_1^2 + \lambda_{345} v_2^2 \\ m_{22}^2 &= -\text{Re}(m_{12}^2) \frac{v_1}{v_2} + \lambda_2 v_2^2 + \lambda_{345} v_1^2 \\ \text{Im}(m_{12}^2) &= v_1 v_2 \text{Im}(\lambda_5), \end{aligned} \quad (3)$$

where  $\lambda_{345} = \lambda_3 + \lambda_4 + \text{Re}(\lambda_5)$ . With our conventions,  $v = \sqrt{v_1^2 + v_2^2} = (\sqrt{2}G_\mu)^{-1/2} = 246$  GeV. Thus,  $v_1$  and  $v_2$  depend only on  $\tan\beta = v_2/v_1$ .

We denote by “ $Z_2$  basis”, the basis where the Higgs potential has the form in Eq. (1) and the vevs are given by Eq. (2), and we parametrize the fields in this basis by

$$\phi_1 = \begin{pmatrix} \varphi_1^+ \\ \frac{1}{\sqrt{2}}(v_1 + \eta_1 + i\chi_1) \end{pmatrix}, \quad \phi_2 = \begin{pmatrix} \varphi_2^+ \\ \frac{1}{\sqrt{2}}(v_2 + \eta_2 + i\chi_2) \end{pmatrix}. \quad (4)$$

The charged fields are changed into the mass basis by

$$\begin{aligned} G^+ &= \cos\beta \varphi_1^+ + \sin\beta \varphi_2^+, \\ H^+ &= -\sin\beta \varphi_1^+ + \cos\beta \varphi_2^+. \end{aligned} \quad (5)$$

We apply the same transformation to the imaginary parts of the neutral fields,

$$\begin{aligned} G^0 &= \cos\beta \chi_1 + \sin\beta \chi_2, \\ \eta_3 &= -\sin\beta \chi_1 + \cos\beta \chi_2, \end{aligned} \quad (6)$$

but *not* to the real parts of the neutral fields [18, 19]. As shown below, this is done in order to keep a clean definition for the angles  $\alpha_i$  leading the neutral fields from the  $Z_2$  basis directly into their mass basis<sup>1</sup>.  $G^+$  and  $G^0$  are the

---

<sup>1</sup> Recall that  $\beta$  is the angle leading from the  $Z_2$  basis into the Higgs basis. In the completely  $Z_2$  symmetric case,  $\alpha - \beta$  is the angle leading from the Higgs basis into the mass basis, and (thus)  $\alpha$  is the angle leading directly from the  $Z_2$  basis into the mass basis.

would-be Goldstone bosons and  $H^+$  is already the physical charged Higgs field, with mass  $m_{H^\pm}$ . Finally, one needs to diagonalize the (squared) mass matrix for the neutral fields  $\mathcal{M}^2$ , whose components are

$$(\mathcal{M}^2)_{ij} = \frac{\partial^2 V_H}{\partial \eta_i \partial \eta_j}. \quad (7)$$

This is achieved through an orthogonal transformation

$$\begin{pmatrix} h_1 \\ h_2 \\ h_3 \end{pmatrix} = R \begin{pmatrix} \eta_1 \\ \eta_2 \\ \eta_3 \end{pmatrix}, \quad (8)$$

such that

$$R \mathcal{M}^2 R^T = \text{diag} (m_1^2, m_2^2, m_3^2), \quad (9)$$

and  $m_1 \leq m_2 \leq m_3$  are the masses of the neutral Higgs particles. The matrix  $R$  may be parametrized by [9]

$$R = \begin{pmatrix} c_1 c_2 & s_1 c_2 & s_2 \\ -(c_1 s_2 s_3 + s_1 c_3) & c_1 c_3 - s_1 s_2 s_3 & c_2 s_3 \\ -c_1 s_2 c_3 + s_1 s_3 & -(c_1 s_3 + s_1 s_2 c_3) & c_2 c_3 \end{pmatrix} \quad (10)$$

with  $s_i = \sin \alpha_i$  and  $c_i = \cos \alpha_i$  ( $i = 1, 2, 3$ ). Without loss of generality, the angles may be varied in the intervals [9]

$$-\pi/2 < \alpha_1 \leq \pi/2, \quad -\pi/2 < \alpha_2 \leq \pi/2, \quad 0 \leq \alpha_3 \leq \pi/2. \quad (11)$$

The lightest neutral Higgs particle (the putative 125 GeV state) is determined by the first row of  $R$ . If  $|s_2| = 0$ , then  $\eta_3$  does not contribute to  $h_1$ , which is a pure scalar. Notice that, in this case, there may be CP violation due to mixing in the  $h_2, h_3$  states [20]. This possibility will affect CP violating observables but not the current known data. If  $|s_2| = 1$ , then only  $\eta_3$  contributes to  $h_1$ , which is a pure pseudoscalar. In this case there is CP conservation. We conclude that

$$|s_2| = 0 \Rightarrow h_1 \text{ is a pure scalar}, \quad (12)$$

$$|s_2| = 1 \Rightarrow h_1 \text{ is a pure pseudoscalar}, \quad (13)$$

and  $|s_2|$  is a measure of the pseudoscalar content of the lightest Higgs scalar.

Given Eqs. (3), the scalar sector depends only on the eight parameters  $\beta$ ,  $\text{Re}(m_{12}^2)$ ,  $\text{Im}(m_{12}^2)$ ,  $\lambda_{1,2,3,4}$ , and  $\text{Re}(\lambda_5)$ . As suggested in Ref. [10], these can be traded for  $m_1$ ,  $m_2$ ,  $m_{H^\pm}$ ,  $\alpha_{1,2,3}$ ,  $\beta$ , and  $\text{Re}(m_{12}^2)$ . In this approach,  $m_3$  is a derived quantity, given by

$$m_3^2 = \frac{m_1^2 R_{13}(R_{12} \tan \beta - R_{11}) + m_2^2 R_{23}(R_{22} \tan \beta - R_{21})}{R_{33}(R_{31} - R_{32} \tan \beta)}. \quad (14)$$

The implementation of the  $Z_2$  symmetry in the fermion sector means that each fermion type (up quark, down quark, and charged leptons) can couple only to one of the original scalar doublets. As an example, let us consider three down type quarks coupling exclusively to  $\phi_1$ . We start from the Yukawa lagrangian

$$-\mathcal{L}_Y = \bar{q}_L \Gamma_1 \phi_1 n_R + \text{h.c.}, \quad (15)$$

where  $q_L^T = (p_L, n_L)$  is a left-handed doublet of the gauge group, having 3 components in family space, while  $n_R$  has 3 down type quarks, each a singlet under the gauge group.  $\Gamma_1$  is the  $3 \times 3$  matrix of Yukawa couplings, and h.c. stands for hermitian conjugation. After SSB, the lagrangian has a piece involving the neutral component of  $\phi_1$ , which may be written as

$$\bar{n}_L \Gamma_1 \frac{v_1}{\sqrt{2}} \left[ 1 + \frac{\eta_1 + i\chi_1}{v_1} \right] n_R + \text{h.c.} = \bar{d}_L M_d d_R + \bar{d}_L \frac{M_d}{v_1} (\eta_1 + i\chi_1) d_R + \text{h.c.} \quad (16)$$

To obtain the last expression we have rotated the fields  $n_L$  and  $n_R$  into the mass basis ( $d_L$  and  $d_R$ ), diagonalizing the matrix  $\Gamma_1 v_1 / \sqrt{2}$  to obtain the (diagonal) down quark mass matrix  $M_d$ . Now, we need

$$\begin{aligned} \eta_1 \pm i\chi_1 &= (R_{k1} \mp i s_\beta R_{k3}) h_k \pm i c_\beta G^0, \\ \eta_2 \pm i\chi_2 &= (R_{k2} \pm i c_\beta R_{k3}) h_k \pm i s_\beta G^0, \end{aligned} \quad (17)$$

	Type I	Type II	Lepton Specific	Flipped
Up	$\frac{R_{12}}{s_\beta} - ic_\beta \frac{R_{13}}{s_\beta}$	$\frac{R_{12}}{s_\beta} - ic_\beta \frac{R_{13}}{s_\beta}$	$\frac{R_{12}}{s_\beta} - ic_\beta \frac{R_{13}}{s_\beta}$	$\frac{R_{12}}{s_\beta} - ic_\beta \frac{R_{13}}{s_\beta}$
Down	$\frac{R_{12}}{s_\beta} + ic_\beta \frac{R_{13}}{s_\beta}$	$\frac{R_{11}}{c_\beta} - is_\beta \frac{R_{13}}{c_\beta}$	$\frac{R_{12}}{s_\beta} + ic_\beta \frac{R_{13}}{s_\beta}$	$\frac{R_{11}}{c_\beta} - is_\beta \frac{R_{13}}{c_\beta}$
Leptons	$\frac{R_{12}}{s_\beta} + ic_\beta \frac{R_{13}}{s_\beta}$	$\frac{R_{11}}{c_\beta} - is_\beta \frac{R_{13}}{c_\beta}$	$\frac{R_{11}}{c_\beta} - is_\beta \frac{R_{13}}{c_\beta}$	$\frac{R_{12}}{s_\beta} + ic_\beta \frac{R_{13}}{s_\beta}$

TABLE I: Couplings of the fermions to the lightest scalar,  $h_1$ , presented, for each case, in the form  $a + ib$ .

which were obtained by inverting Eqs. (6) and (8), and where a sum over  $k = 1, 2, 3$  is implied. The couplings with the neutral scalar particles are obtained substituting Eq. (17) in Eq. (16) to get

$$\bar{d}_L \frac{M_d}{v_1} (R_{k1} - is_\beta R_{k3}) h_k d_R + \text{h.c.} = \bar{d}_L \frac{M_d}{v} \left( \frac{R_{k1}}{c_\beta} - is_\beta \frac{R_{k3}}{c_\beta} \gamma_5 \right) d_R h_k. \quad (18)$$

We are interested in the couplings of the fermions to the lightest scalar  $h_1$ . Comparing with the notation of the effective lagrangian (A1) in the appendix, needed for our calculations, we obtain

$$a = \frac{R_{11}}{c_\beta}, \quad b = -s_\beta \frac{R_{13}}{c_\beta} \quad (\text{down type quarks couple to } \phi_1). \quad (19)$$

A similar analysis leads to Table I. Notice that  $s_2 = 0$  implies  $R_{13} = 0$ , in which case all  $b$  coefficients in Table I vanish, confirming that  $h_1$  couples to the fermions as a pure scalar, and vindicating Eq. (12). Similarly,  $|s_2| = 1$  leads to  $R_{11} = 0 = R_{12}$ , and all  $a$  coefficients in Table I vanish, implying that  $h_1$  couples to the fermions with  $i\gamma_5$ , being a pure pseudoscalar, as stated in Eq. (13).

In Model I, all quarks and charged leptons couple to the doublet  $\phi_2$ , and the corresponding coupling factors can be read from the first column of Table I. In Model II, the up quarks still couple to  $\phi_2$  but the remaining fermions couple to  $\phi_1$  - the respective couplings are shown in the second column of Table I. The Lepton-Specific and Flipped models discussed in Refs. [15, 16] would be obtained by taking for the charged leptons the opposite choice taken for the down quarks. We have checked that our results reproduce those for Model II included in Ref. [14].

Expanding the covariant derivative terms of the neutral scalars, the triple interactions of  $h_1$  with  $WW$  and  $ZZ$  may be written as in Eq. (A3), with

$$C = c_\beta R_{11} + s_\beta R_{12}. \quad (20)$$

As expected, when  $|s_2| = 1$ ,  $R_{11} = 0 = R_{12}$  and there is no tree-level coupling of the pure pseudoscalar  $h_1$  to a pair of gauge bosons. From the Higgs potential, we may get the triple vertex of  $h_1$  with the charged Higgs bosons as in Eq. (A2), with

$$-\lambda = c_\beta [s_\beta^2 \lambda_{145} + c_\beta^2 \lambda_3] R_{11} + s_\beta [c_\beta^2 \lambda_{245} + s_\beta^2 \lambda_3] R_{12} + s_\beta c_\beta \text{Im}(\lambda_5) R_{13}, \quad (21)$$

where  $\lambda_{145} = \lambda_1 - \lambda_4 - \text{Re}(\lambda_5)$  and  $\lambda_{245} = \lambda_2 - \lambda_4 - \text{Re}(\lambda_5)$ . In the pure pseudoscalar limit, only the last term of Eq. (21) survives, showing that a pure pseudoscalar can only couple to a pair of charged scalars if there is explicit CP violation in the scalar potential, through  $\text{Im}(\lambda_5)$ .

For a given set of input parameters, the effective couplings ( $a$ ,  $b$ ,  $C$ , and  $\lambda$ ) discussed in this section can be used on the equations in appendix A in order to find the production rates for  $h_1$  and its decay rates into all final states. For each final state  $f$ , we define the ratio

$$R_f = \frac{\sigma(pp \rightarrow h_1) \text{BR}(h_1 \rightarrow f)}{\sigma(pp \rightarrow h)_{\text{SM}} \text{BR}(h \rightarrow f)_{\text{SM}}}, \quad (22)$$

where  $\sigma(pp \rightarrow h_1)$  is an inclusive production rate obtained by summing over production mechanisms of  $h_1$ , and  $\text{BR}(h_1 \rightarrow f)$  is the branching ratio of the decay of  $h_1$  into the final state  $f$ .

The production mechanisms included in  $\sigma(pp \rightarrow h_1)$  include: the usual gluon-gluon fusion processes (which involve loops with both top and bottom quarks); vector boson fusion (VBF) processes; so-called associated production processes, with a  $W$  or  $Z$  boson in the final state, alongside  $h_1$ ; and the  $b\bar{b} \rightarrow h_1$  process as well. An important point needs to be explained at this juncture: since  $h_1$  is a mix of scalar and pseudoscalar states, its production mechanism will involve, likewise, a mix of production rates pertaining to a scalar and a pseudoscalar particle. For instance, a pure

pseudoscalar particle has no VBF or associated production mechanisms; on the other hand, due to different fermion couplings, the gluon-gluon fusion cross section is different for production of a scalar or pseudoscalar states of the same mass. The exact formulae for  $\sigma(pp \rightarrow h_1)$  can be found in Appendix A. Using those formulae we were able to express the production factors in terms of next-to-leading order cross sections for each of the mechanisms considered, calculated using HIGLU [21] for the gluon-gluon cross section,  $bb@nnlo$  [22] for the  $b\bar{b}$  process and reference [23] (and references therein), for the remaining processes, all multiplied by the adequate factors pertaining to the mixing of scalar-pseudoscalar states.

The branching ratios  $BR(h_1 \rightarrow f)$  also need to be computed considering the mixed nature of the  $h_1$  state, and the relevant formulae can be found in Appendix A. Notice that, since the branching ratio is the partial width divided by the sum of all decay widths, a parameter choice that affects, for example,  $h_1 \rightarrow b\bar{b}$  will have an impact on  $R_{\gamma\gamma}$  because it affects the overall decay width.

We are particularly interested on what one can learn from the current LHC bounds on  $R_{\gamma\gamma}$ ,  $R_{ZZ}$ ,  $R_{WW}$ , and  $R_{b\bar{b}}$ . These are combined with other known constraints, including recent results from the Tevatron [24, 25]. In this analysis, we utilize the explicit bounds obtained for the several  $R_f$  from the experimental data by Espinosa *et al.* [26]. Specifically, we use their Table III, updated after Moriond 2012. Similar summaries of the experimental bounds have been obtained in Refs. [27–29]. Since the current errors are large, we are not interested so much in the precise values but rather in the qualitative features hinted at by current bounds. Surprisingly, we can already exclude very large regions of the 2HDM parameter space, and place constraints on the pseudoscalar content of the lightest Higgs particle.

### III. ANALYSIS AND RESULTS

We performed an extensive scan of the 8-dimensional parameter space of the models we are studying. Our fixed inputs are  $v = 246$  GeV and  $m_1 = 125$  GeV. We then took random values of: the angles  $\alpha_1$ ,  $\alpha_2$  and  $\alpha_3$  in their allowed intervals of variation, specified in Eq. (11);  $\tan\beta$  between 1 and 30; the masses  $m_2$  (above the value of  $m_1$ ) and  $m_{H^\pm}$ , the latter with values above 90 GeV; and  $\text{Re}(m_{12}^2)$ , taken in the range from  $-10^6$  to  $+10^6$  GeV<sup>2</sup>.

The charged Higgs couplings to the fermions have exactly the same form as the ones in a softly broken  $Z_2$  symmetric two-Higgs doublet model. Therefore the bounds derived for the charged sector still hold for the CP-violating scenario under study. The LEP  $R_b$  constraint (from  $Z \rightarrow b\bar{b}$ ) excludes values of  $\tan\beta < 1$  even in the CP violating scenario. One should note that although the expressions for  $R_b$  change in the CP-violating scenario, the main contributions for low  $\tan\beta$  come from the charged Higgs diagrams [11, 30]. Constraints from B-physics, and particularly those coming from  $b \rightarrow s\gamma$  [31–36], have excluded a charged Higgs boson mass below 300 GeV in models type II and Flipped, almost independently of  $\tan\beta$ . Charged Higgs bosons with masses as low as 100 GeV are instead still allowed in models Type I and Lepton-Specific [37–39]. Finally  $b \rightarrow s\gamma$  implies  $\tan\beta > 1$  for a charged Higgs mass below approximately 600 GeV.

Once a given set of parameters is chosen, a value for  $m_3^2$  is computed from Eq. (14). If that value is positive and larger than  $m_2^2$ , we then verify that all theoretical constraints on the potential are satisfied. The quartic couplings  $\lambda_{1\dots 5}$  are computed using the formulae in Eq. (B.1) from Ref. [14]. One then verifies whether these quartic couplings obey the conditions which ensure that the potential is bounded from below and that unitarity and perturbativity are satisfied - Eqs. (2.20) and (2.21) from Ref. [14], respectively. Finally, one verifies that the potential's parameters are such that the current constraints on the  $S$ ,  $T$  and  $U$  oblique parameters are obeyed. To do so, we have used the formulae presented in Appendix D of Ref. [6]. If all of these constraints are obeyed, the set of parameters (a “point” in parameter space) is deemed satisfactory and one then proceeds to calculate the branching ratios and production factors of the  $h_1$  state.

#### A. Model I

In Model I, as was explained earlier, all fermions couple to the same doublet,  $\phi_2$  by convention. The couplings between  $h_1$  and the fermions are affected by the  $a$  and  $b$  parameters shown in eq. (A1) which, for this model and the  $\tan\beta$  we chose, tend to be smaller than 1. We generated over 270000 points for this model.

In Fig. 1, we show how the  $R_{\gamma\gamma} - R_{ZZ}$  plane is filled by Model I, for three selections of points: points for which one has an  $h_1$  state which is essentially a scalar (*i.e.*, for which the angle  $\alpha_2$  obeys  $|s_2| < 0.1$ ); an  $h_1$  state with  $0.45 < |s_2| < 0.55$ ; and points for which  $h_1$  is essentially a pseudoscalar ( $|s_2| > 0.83$ ). There are several salient features. First, we notice that even the current rather loose bounds already kill large regions of the model's parameter space. In particular,  $R_{ZZ}$  tends to be smaller than 1 in Model I, for any values of the parameters of the model. Second, a large pseudoscalar component ( $|s_2| > 0.83$ ) is already excluded, both by the  $ZZ$  bounds and by the  $\gamma\gamma$

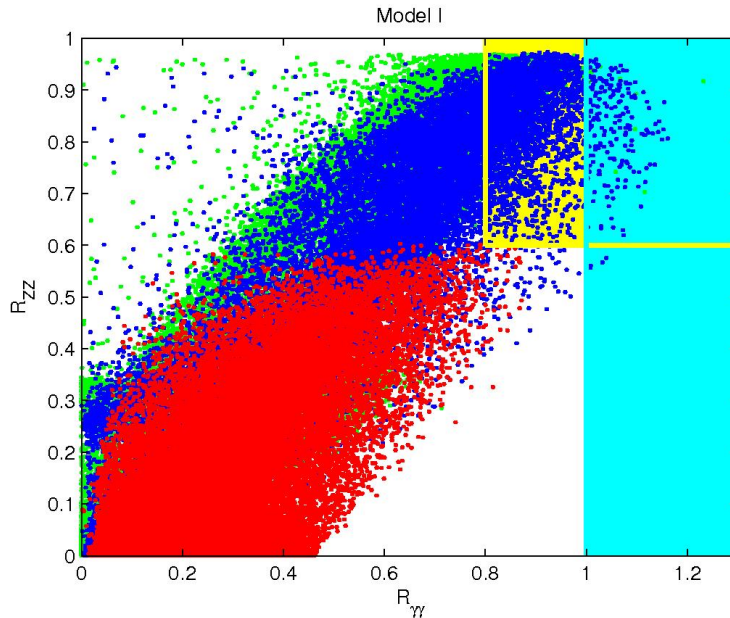


FIG. 1: Scatter plot in the  $R_{\gamma\gamma} - R_{ZZ}$  plane for the type I 2HDM. The color coded points have the following correspondences: green (light grey) means  $|s_2| < 0.1$  ( $h_1$  is mostly scalar), blue (black) means  $0.45 < |s_2| < 0.55$ , and red (dark grey) means  $|s_2| > 0.83$  ( $h_1$  is mostly pseudoscalar). The yellow and light blue (light grey and grey) bands shows the current ATLAS and CMS bounds, from Ref. [26].

bounds. That the  $ZZ$  bounds constrain  $s_2$  was expected and was the primary motivation for this work. Indeed, when  $|s_2| = 1$ , Eq. (20) leads to  $C = 0$ , guaranteeing that there is no coupling of  $h_1$  to  $ZZ$  nor to  $WW$ . What is new is that, in this model, the known experimental bounds and theoretical constraints make  $|s_2| \sim 1$  inconsistent with  $R_{\gamma\gamma}$  *even if  $R_{ZZ}$  vanished*. A third important point (not clearly visible in Fig. 1) is that the  $0.45 < |s_2| < 0.55$  (blue/black) region extends further into the  $R_{\gamma\gamma}$  experimentally allowed region than the  $|s_2| < 0.1$  (green/light grey) region<sup>2</sup>. This has the following implication: if the current ATLAS central values for  $R_{\gamma\gamma}$  remain as the errors get smaller, then the model seems to prefer a mixture of scalar and pseudoscalar components in the lowest lying Higgs particle. Finally, we find that only for  $|s_2| < 0.83$  do we start to get points inside the band allowed by current experiments.

We have mentioned that there are very few points above around  $R_{\gamma\gamma} = 1$  corresponding to the (almost) pure scalar solution  $|s_2| < 0.1$ . There are quite a few more points in the large  $R_{\gamma\gamma}$  region corresponding to  $0.45 < |s_2| < 0.55$ . Fig. 1 shows that the former tend to concentrate around  $R_{ZZ} \sim 0.8$ . A better handle on the difference between  $|s_2| < 0.1$  and  $0.45 < |s_2| < 0.55$  is provided by  $R_{b\bar{b}}$ , as shown in Fig. 2, where Model I's results are presented in the  $R_{\gamma\gamma} - R_{b\bar{b}}$  plane. We see that the pure scalar solution with large  $R_{\gamma\gamma}$  leads to  $R_{b\bar{b}} \sim 1$ , while the large values of  $R_{\gamma\gamma}$  correspond to  $R_{b\bar{b}} \sim 0.5$  when  $0.45 < |s_2| < 0.55$ . Thus, as the errors get smaller, a comparison between  $R_{\gamma\gamma}$ ,  $R_{ZZ}$ , and  $R_{b\bar{b}}$  can be used to further constrain  $|s_2|$  in Model I.

Regarding the current bounds on  $R_{b\bar{b}}$ , Espinosa *et al* [26] provide an LHC interval of  $R_{b\bar{b}} < 3.3$ , which spans the entire range for this variable displayed in Fig. 2. In that reference there is also a bound stemming from Tevatron data,  $1.3 < R_{b\bar{b}}^{TEVATRON} < 2.8$ ; once translated into LHC bounds for Model I - that is, with the appropriate LHC production factors - this would give approximately  $R_{b\bar{b}} > 1.2$  in Fig. 2. This would eliminate most of the available parameter space left by the bounds on  $R_{\gamma\gamma}$ . Accurate measurements of  $R_{b\bar{b}}$  are thus of extreme importance for this model.

We have also looked at  $h_1 \rightarrow W^+W^-$ . Notice that, within our tree-level calculations, and even for a mixed  $h_1$  state,  $R_{WW} \simeq R_{ZZ}$ , since we are dealing with ratios to SM quantities. As such, one can glean information about  $R_{WW}$  from the plot in Fig. 1. After an earlier central value compatible with the SM, ATLAS presented at Moriond

<sup>2</sup> Please notice that there is some superposition of points in several regions, so that “underneath” the points shown in blue/black, for instance, there may well exist green/light grey points. This is common to all figures shown in this work.

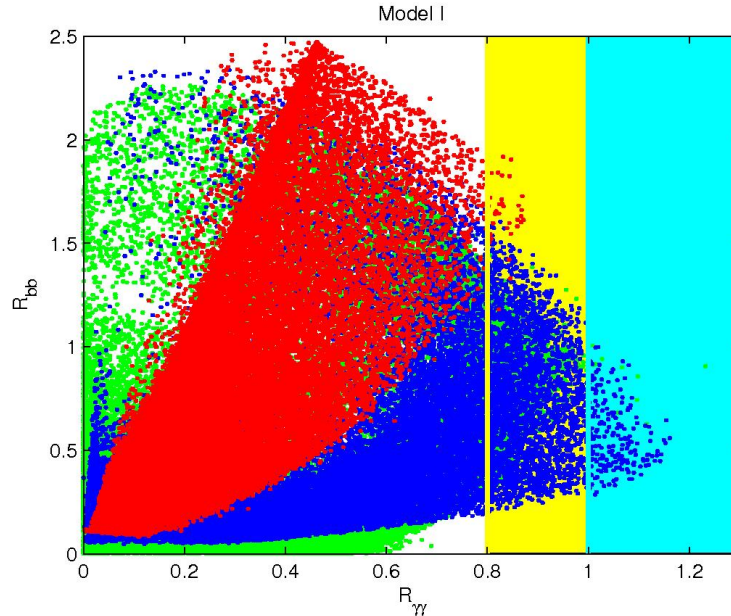


FIG. 2: Scatter plot in the  $R_{\gamma\gamma} - R_{b\bar{b}}$  plane for the type I 2HDM. The color codes are the same as the previous figure's.

2012 results which are now slightly over one sigma smaller than the SM – compare the respective entries in Tables I and III of Ref. [26]. Their Moriond 2012 bounds impose  $R_{WW}$  smaller than 0.8 for ATLAS and 1 for CMS. If this situation were to remain as errors get smaller, then the SM itself would be in trouble. As seen in Fig. 1 for  $h_1 \rightarrow ZZ$  in Model I, the values for  $h_1 \rightarrow W^+W^-$  are smaller than one, enabling a possible accommodation of a low  $R_{WW}$  signal.

## B. Model II

We now turn to Model II. As explained, in this model the down-type quarks and charged leptons couple to the  $\phi_1$  doublet, and the up-type quarks couple to  $\phi_2$ . The corresponding couplings can be read off Table I, and we see that the bottom quark couplings are proportional to  $1/\cos\beta$ . As such, one can expect, in this model, an enhancement of the production of  $h_1$  via the gluon-gluon fusion  $b$ -quark triangle, or the  $b\bar{b} \rightarrow h_1$  channel for large values of  $\tan\beta$ . Similarly, the branching ratio  $BR(h_1 \rightarrow b\bar{b})$  will also reach higher values than in Model I for large  $\tan\beta$ . As was mentioned earlier, in Model II there are stringent constraints on the value of the charged Higgs mass - it needs to be larger than about 300 GeV - stemming from  $b \rightarrow s\gamma$  data. We included that cut in our scan of this model's parameter space, and again we generated over 270000 points for this model.

In Fig. 3 we show our results for Model II in the  $R_{\gamma\gamma} - R_{ZZ}$  plane, while Fig. 4 shows the results in the  $R_{\gamma\gamma} - R_{b\bar{b}}$  plane. As expected, large values of  $|s_2|$  are excluded by the  $ZZ$  bound. There are similarities and differences between the two models. The striking feature that  $R_{\gamma\gamma}$  by itself constrains  $|s_2|$  is common to models I and II, and in both cases  $|s_2|$  is found to have to be smaller than about 0.83.

The most noticeable difference between both models is that Model I keeps roughly  $R_{\gamma\gamma} < 2$ ,  $R_{ZZ} < 1$ , and  $R_{b\bar{b}} < 2.5$  while, in Model II, values as large as  $R_{\gamma\gamma} < 2.5$ ,  $R_{ZZ} < 2.7$ , and  $R_{b\bar{b}} > 2.5$ <sup>3</sup> are allowed. Also, in Model II, the  $|s_2| < 0.1$  (green/light grey) region extends further into the  $R_{\gamma\gamma}$  experimentally allowed region than the  $0.45 < |s_2| < 0.55$  (blue/black) region. This is the opposite of what we observe in Model I. Finally, we see from Fig. 4 that the pure scalar solution with large  $R_{\gamma\gamma}$  tends to imply  $R_{b\bar{b}} < 1$ , while the large values of  $R_{\gamma\gamma}$  correspond to  $R_{b\bar{b}} > 1$  when  $0.45 < |s_2| < 0.55$ . Thus, as better measurements are available,  $R_{b\bar{b}}$  might become instrumental

<sup>3</sup> Values as high as 10 for  $R_{b\bar{b}}$  were found, for extremely small values of  $R_{\gamma\gamma}$ , though they are not displayed in the plot of Fig. 4 for ease of presentation. These high values correspond to both the gauge-phobic limit of this model and the enhancement with large  $\tan\beta$  alluded to earlier.

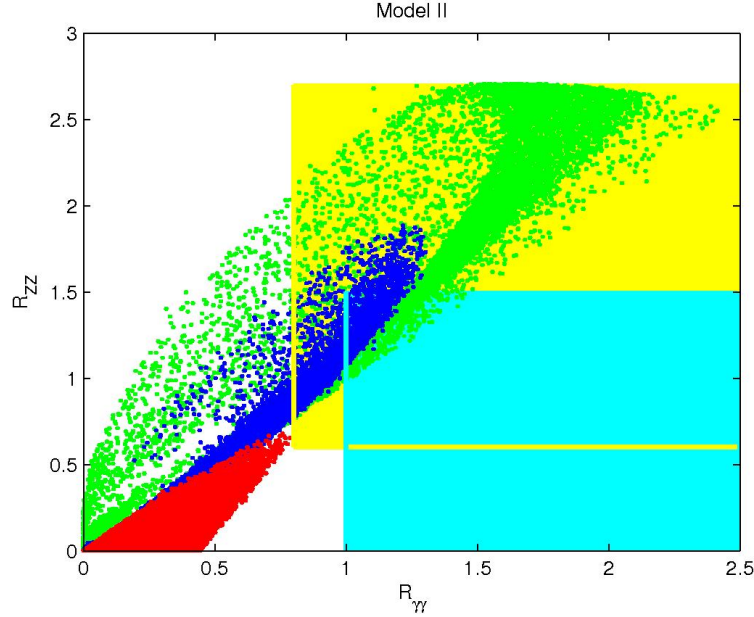


FIG. 3: Scatter plot in the  $R_{\gamma\gamma} - R_{ZZ}$  plane for the type II 2HDM. The color codes are the same as previous figures'.

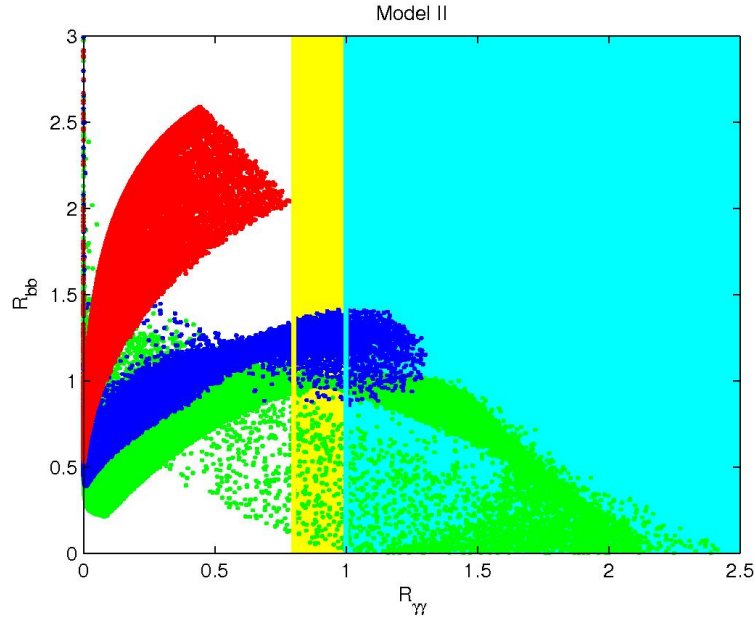


FIG. 4: Scatter plot in the  $R_{\gamma\gamma} - R_{b\bar{b}}$  plane for the type II 2HDM. The color codes are the same as previous figures'.

in constraining  $s_2$ . In fact, the current Tevatron bounds, cited by [26], translated into LHC for Model II, would give roughly  $1.1 < R_{b\bar{b}} < 2.8$ , which, if confirmed, would exclude an extremely significant portion of this model's parameter space. In particular, it would seem to disfavor the possibility of  $h_1$  being a pure scalar.

Finally, a word on the constraints emerging from  $R_{WW}$  for this model. As mentioned above for the Model I analysis, current ATLAS and CMS bounds favor values of  $R_{WW}$  smaller than 1 - since  $R_{WW} \simeq R_{ZZ}$ , we can see from Fig. 3 that that region is heavily disfavoured for Model II by the current bounds on  $R_{\gamma\gamma}$ . As a result, very low experimental values for  $R_{WW}$  will exclude the SM and also the type II model.



## IV. CONCLUSIONS

With the LHC providing physicists with a wealth of data, and the first hints of the existence of a Higgs particle with a mass around 125 GeV, it becomes possible to constrain, not only the SM but also extensions of it, such as the 2HDM. Previous studies considered the possibility that the LHC might be observing a pure scalar, or a pure pseudoscalar. We have considered the possibility that the putative scalar candidate at the LHC is a mixed state, neither scalar nor pseudoscalar. We considered a specific model, a version of the 2HDM with a  $Z_2$  discrete symmetry which has been softly broken, such that the model has explicit CP violation in the scalar sector. The degree of “pseudoscalarity” of the lightest scalar  $h_1$  is measured by a mixing angle  $\alpha_2$  such that  $|s_2| = |\sin \alpha_2| \simeq 1$  corresponds to a pure pseudoscalar state (and  $|s_2| \simeq 0$  to a pure scalar one). We considered two specific extensions of the  $Z_2$  symmetry to the fermionic sector, the so-called Models I and II, which have very different phenomenologies.

We have computed the production rate of  $h_1$  times its branching ratio into several final states -  $R_f$  - relative to the expected values for such observables in the SM. We have shown that this version of the 2HDM can do at least as good a job as the SM in fitting the current data. But we have also shown that even the current loose bounds on  $R_{\gamma\gamma}$  and  $R_{ZZ}$  already put severe constraints on the parameter space of these versions of the 2HDM. In particular, our work suggests that if current trends in the values of  $R_{WW}$  at the LHC, as well as in the Tevatron data on  $R_{b\bar{b}}$ , persist, the versions of the 2HDM herein considered might have a hard time reproducing the data. However, if that were the case, the SM would also be in trouble. Current data forces  $|s_2| < 0.83$ , a constraint which holds roughly even if one considers only the  $R_{\gamma\gamma}$  bound. This by itself excludes a large pseudoscalar component.

## Acknowledgments

We are grateful to A. Arhrib for discussions pertaining to his related study [44]. We thank Renato Guedes for help with HIGLU. J.P.S. is grateful to J.C. Romão for useful discussions. This work is supported in part by the Portuguese *Fundação para a Ciência e a Tecnologia* (FCT) under contract PTDC/FIS/117951/2010 and by an FP7 Reintegration Grant, number PERG08-GA-2010-277025. P.M.F. and R.S. are also partially supported by PEst-OE/FIS/UI0618/2011. The work of J.P.S. is also funded by FCT through the projects CERN/FP/109305/2009 and U777-Plurianual, and by the EU RTN project Marie Curie: PITN-GA-2009-237920.

**Note added:** While writing this paper, Ref. [45] appeared discussing a complementary and interesting feature of the type I model: the production and detection of its charged Higgs.

- 
- [1] G. Aad *et al.* [ATLAS Collaboration], Phys. Lett. B **710**, 49 (2012) [arXiv:1202.1408 [hep-ex]].
  - [2] S. Chatrchyan *et al.* [CMS Collaboration], arXiv:1202.1488 [hep-ex].
  - [3] G. Burdman, C. Haluch, and R. Matheus, arXiv:1112.3961 [hep-ph].
  - [4] E. Cervero and J. -M. Gerard, arXiv:1202.1973 [hep-ph].
  - [5] M. T. Frandsen and F. Sannino arXiv:1203.3988 [hep-ph].
  - [6] For a comprehensive review see, for example, G. C. Branco, P. M. Ferreira, L. Lavoura, M. N. Rebelo, M. Sher, and J. P. Silva, to appear in Phys. Rept. arXiv:1106.0034 [hep-ph].
  - [7] I. F. Ginzburg, M. Krawczyk and P. Osland, hep-ph/0211371.
  - [8] W. Khater and P. Osland, Nucl. Phys. B **661**, 209 (2003) [hep-ph/0302004].
  - [9] A. W. El Kaffas, P. Osland and O. M. Ogreid, Nonlin. Phenom. Complex Syst. **10**, 347 (2007) [hep-ph/0702097 [HEP-PH]].
  - [10] A. W. El Kaffas, W. Khater, O. M. Ogreid, and P. Osland, Nucl. Phys. B **775**, 45 (2007) [hep-ph/0605142].
  - [11] A. Wahab El Kaffas, P. Osland and O. M. Ogreid, Phys. Rev. D **76**, 095001 (2007) [arXiv:0706.2997 [hep-ph]].
  - [12] P. Osland, P. N. Pandita and L. Selbuz, Phys. Rev. D **78**, 015003 (2008) [arXiv:0802.0060 [hep-ph]].
  - [13] B. Grzadkowski and P. Osland, Phys. Rev. D **82**, 125026 (2010) [arXiv:0910.4068 [hep-ph]].
  - [14] A. Arhrib, E. Christova, H. Eberl and E. Ginina, JHEP **1104**, 089 (2011) [arXiv:1011.6560 [hep-ph]].
  - [15] P. M. Ferreira, R. Santos, M. Sher and J. P. Silva, to appear in Phys. Rev. D, arXiv:1112.3277 [hep-ph].
  - [16] P. M. Ferreira, R. Santos, M. Sher and J. P. Silva, Phys. Rev. D **85**, 035020 (2012) [arXiv:1201.0019 [hep-ph]].
  - [17] G. C. Branco, L. Lavoura and J. P. Silva, “*CP Violation*”, Oxford University Press, Int. Ser. Monogr. Phys. **103** (1999) 1.
  - [18] Applying the same transformations to the real parts of the neutral fields (and, thus, to all fields) would lead us into the Higgs basis [17, 19]:

$$\begin{pmatrix} H_1 \\ H_2 \end{pmatrix} = \begin{pmatrix} c_\beta & s_\beta \\ -s_\beta & c_\beta \end{pmatrix} \begin{pmatrix} \phi_1 \\ \phi_2 \end{pmatrix}, \quad (23)$$

with

$$H_1 = \begin{pmatrix} G^+ \\ \frac{1}{\sqrt{2}}(v + H^0 + iG^0) \end{pmatrix}, \quad H_2 = \begin{pmatrix} H^+ \\ \frac{1}{\sqrt{2}}(R_2 + iI_2) \end{pmatrix}. \quad (24)$$

The relation between the scalar fields is

$$\begin{pmatrix} \eta_1 \\ \eta_2 \\ \eta_3 \end{pmatrix} = R_H \begin{pmatrix} H^0 \\ R_2 \\ I_2 \end{pmatrix} = \begin{pmatrix} c_\beta & -s_\beta & 0 \\ s_\beta & c_\beta & 0 \\ 0 & 0 & 1 \end{pmatrix} \begin{pmatrix} H^0 \\ R_2 \\ I_2 \end{pmatrix}, \quad (25)$$

leading to

$$\begin{pmatrix} h_1 \\ h_2 \\ h_3 \end{pmatrix} = R \begin{pmatrix} \eta_1 \\ \eta_2 \\ \eta_3 \end{pmatrix} = R R_H \begin{pmatrix} H^0 \\ R_2 \\ I_2 \end{pmatrix}. \quad (26)$$

The matrix  $T = R_H^T R^T$  is needed in Eq. (381) of Ref. [6], in order to compute the bounds from the oblique radiative corrections in Eqs. (388) and (393) of [6].

- [19] L. Lavoura, J. P. Silva, Phys. Rev. D **50**, 4619 (1994); F. J. Botella and J. P. Silva, Phys. Rev. D **51**, 3870 (1995).  
 [20] Lavoura and Silva [19] have classified all basis invariant measures of CP violation which can occur in the scalar sector of the 2HDM. In particular, for  $s_2 = 0$  and using [18], we can show that the invariant in Eq. (331) of Ref. [6] is proportional to

$$J_1 \propto (m_1^2 - m_2^2)(m_1^2 - m_3^2)(m_2^2 - m_3^2) \cos(\beta - \alpha_1) \sin^2(\beta - \alpha_1) \cos(\alpha_3) \sin(\alpha_3). \quad (27)$$

Therefore, in general, even if the lightest Higgs is CP even, there can be CP violation in the mixing of the heavier two. This source of CP violation only vanishes if the sine or cosine of  $\beta - \alpha_1$  or of  $\alpha_3$  vanish, or if the heavier two states are degenerate.

- [21] M. Spira, arXiv:hep-ph/9510347.  
 [22] R. V. Harlander and W. B. Kilgore, Phys. Rev. D **68**, 013001 (2003) [hep-ph/0304035].  
 [23] J. Baglio and A. Djouadi, JHEP **1103**, 055 (2011) [arXiv:1012.0530 [hep-ph]].  
 [24] Talks at the Moriond 2012 EW session: CDF Collaboration, CDF Note 10806; D0 Collaboration, D0 Note 6303.  
 [25] [TEVNPH (Tevatron New Phenomena and Higgs Working Group) and CDF and D0 Collaborations], arXiv:1203.3774 [hep-ex].  
 [26] J. R. Espinosa, C. Grojean, M. Muhlleitner and M. Trott, arXiv:1202.3697 [hep-ph].  
 [27] P. P. Giardinio, K. Kannike, M. Raidal and A. Strumia, arXiv:1203.4254 [hep-ph].  
 [28] D. Carmi, A. Falkowski, E. Kuflik and T. Volansky, arXiv:1202.3144 [hep-ph].  
 [29] A. Azatov, R. Contino and J. Galloway, JHEP **1204**, 127 (2012) [arXiv:1202.3415 [hep-ph]].  
 [30] A. W. M. El Kaffas, “Constraining the Two Higgs Doublet Model with CP-Violation,” Ph.D. Thesis (Advisor: Per Osland).  
 [31] W. S. Hou and R. S. Willey, Phys. Lett. B **202** (1988) 591.  
 [32] M. Ciuchini, G. Degrandi, P. Gambino and G. F. Giudice, Nucl. Phys. B **527** (1998) 21.  
 [33] F. Borzumati and C. Greub, Phys. Rev. D **58**, 074004 (1998).  
 [34] F. Borzumati and C. Greub, Phys. Rev. D **59**, 057501 (1999).  
 [35] C. Amsler *et al.* [Particle Data Group Collaboration], Phys. Lett. B **667** (2008) 1.  
 [36] A. Limosani *et al.* [Belle Collaboration], Phys. Rev. Lett. **103** (2009) 241801.  
 [37] M. Aoki, S. Kanemura, K. Tsumura and K. Yagyu, Phys. Rev. D **80** (2009) 015017.  
 [38] H. E. Logan and D. MacLennan, Phys. Rev. D **79** (2009) 115022.  
 [39] S. Su, B. Thomas, Phys. Rev. D **79**, 095014 (2009).  
 [40] A. Djouadi, Phys. Rept. **457**, 1 (2008) [arXiv:hep-ph/0503172].  
 [41] A. Djouadi, Phys. Rept. **459**, 1 (2008) [arXiv:hep-ph/0503173].  
 [42] S. Y. Choi and J. S. Lee, Phys. Rev. D **62**, 036005 (2000) [hep-ph/9912330].  
 [43] S. Y. Choi, K. Hagiwara and J. S. Lee, Phys. Lett. B **529**, 212 (2002) [hep-ph/0110138].  
 [44] A. Arhrib *et al.*, to appear.  
 [45] W. Mader, J.-h. Park, G. M. Pruna, arXiv:1205.2692 [hep-ph].

## Appendix A: Production and decay Rates

In this appendix we present the decay rates for a particle  $h$  with both scalar and pseudoscalar components. The relevant pieces of the Lagrangian are:

$$\mathcal{L}_Y = - \left( \sqrt{2} G_\mu \right)^{\frac{1}{2}} m_f \bar{\psi} (a + ib\gamma_5) \psi h, \quad (A1)$$

$$\mathcal{L}_{hH^+H^-} = \lambda v h H^+ H^-, \quad (A2)$$

$$\mathcal{L}_{hVV} = C \left[ g m_W W_\mu^+ W^{\mu-} + \frac{g}{2c_W} m_Z Z_\mu Z^\mu \right] h, \quad (A3)$$

where  $a$ ,  $b$ , and  $C$  are real,  $c_W = \cos \theta_W$ , and  $\theta_W$  is the Weinberg angle. In the SM,  $a = C = 1$ , and  $b = \lambda = 0$ .

We find:

$$\Gamma(h \rightarrow \gamma\gamma) = \frac{G_\mu \alpha^2 M_h^3}{128 \sqrt{2} \pi^3} \left\{ \left| \sum_f N_c Q_f^2 a A_{1/2}(\tau_f) + C A_1(\tau_W) - \frac{v^2}{2m_{H^\pm}^2} \lambda A_0(\tau_\pm) \right|^2 + \left| \sum_f N_c Q_f^2 b A_{1/2}^A(\tau_f) \right|^2 \right\}, \quad (\text{A4})$$

where  $v = [\sqrt{2}G_\mu]^{-1/2} \approx 246$  GeV and  $m_{H^\pm}$  is the mass of the charged Higgs. For ease of reference, we have used a notation close to that of Djouadi [40, 41], where

$$A_{1/2}(\tau) = 2[\tau + (\tau - 1)f(\tau)]\tau^{-2}, \quad (\text{A5})$$

$$A_{1/2}^A(\tau) = 2\tau^{-1}f(\tau), \quad (\text{A6})$$

$$A_1(\tau) = -[2\tau^2 + 3\tau + 3(2\tau - 1)f(\tau)]\tau^{-2} \quad (\text{A7})$$

$$A_0(\tau) = -[\tau - f(\tau)]\tau^{-2}, \quad (\text{A8})$$

and

$$f(\tau) = \begin{cases} [\arcsin(\sqrt{\tau})]^2 & \tau \leq 1 \\ -\frac{1}{4} \left[ \log \frac{1+\sqrt{1-\tau^{-1}}}{1-\sqrt{1-\tau^{-1}}} - i\pi \right]^2 & \tau > 1 \end{cases}. \quad (\text{A9})$$

The scaling variables are  $\tau_i = M_h^2/(4m_i^2)$ , where  $m_i$  is the mass of the particle in the loop.

Similarly, for the decays into two gluons we find

$$\Gamma(h \rightarrow gg) = \frac{G_\mu \alpha_s^2 M_h^3}{64 \sqrt{2} \pi^3} \left\{ \left| \sum_q a A_{1/2}(\tau_q) \right|^2 + \left| \sum_q b A_{1/2}^A(\tau_q) \right|^2 \right\}, \quad (\text{A10})$$

where the sums run only over quarks  $q$ .

The decays into fermions are given by

$$\Gamma(h \rightarrow f\bar{f}) = N_c \frac{G_\mu m_f^2}{4\sqrt{2}\pi} M_h [a^2 \beta_f^3 + b^2 \beta_f], \quad (\text{A11})$$

where  $\beta_f = \sqrt{1 - 4m_f^2/M_h^2} = \sqrt{1 - \tau^{-1}}$ , while the decays into two vector bosons are given by

$$\Gamma(h \rightarrow V^{(*)}V^{(*)}) = C^2 \Gamma_{\text{SM}}(h \rightarrow V^{(*)}V^{(*)}), \quad (\text{A12})$$

and the partial decay widths in the SM-Higgs case in the two-, three- and four-body approximations,  $\Gamma_{\text{SM}}(h \rightarrow V^{(*)}V^{(*)})$ , can be found in Section I.2.2 of Ref. [40]. Notice that in no decay is there interference between the scalar  $a$  couplings and the pseudoscalar  $b$  couplings.

The same is true in the production mechanisms. We find

$$\sigma(gg \rightarrow h) = \frac{G_\mu \alpha_s^2}{512 \sqrt{2} \pi} \left[ \left| \sum_q a A_{1/2}(\tau) \right|^2 + \left| \sum_q b A_{1/2}^A(\tau) \right|^2 \right], \quad (\text{A13})$$

where the sums, which run over all quarks  $q$ , are dominated by the triangle with top in the loop with, depending on  $\tan \beta$ , relevant contributions from the triangle with bottom in the loop. Therefore, we use

$$\frac{\sigma(gg \rightarrow h)}{\sigma^{\text{SM}}(gg \rightarrow h)} = \frac{|a_t A_{1/2}(\tau_t) + a_b A_{1/2}(\tau_b)|^2 + |b_t A_{1/2}^A(\tau_t) + b_b A_{1/2}^A(\tau_b)|^2}{|A_{1/2}(\tau_t) + A_{1/2}(\tau_b)|^2}. \quad (\text{A14})$$

Similarly,

$$\frac{\sigma_{VBF}}{\sigma_{VBF}^{\text{SM}}} = \frac{\sigma_{VH}}{\sigma_{VH}^{\text{SM}}} = C^2, \quad (\text{A15})$$

and

$$\frac{\sigma(b\bar{b} \rightarrow h)}{\sigma^{\text{SM}}(b\bar{b} \rightarrow h)} = a^2 + b^2. \quad (\text{A16})$$

Notice that these expressions hold for any model with the effective lagrangians of Eqs. (A1)-(A3).

Our results agree with those of Choi *et. al* [42, 43]. For ease of reference, we show their definitions in terms of ours:

$$\begin{aligned} F_{sf}(\tau) &= \frac{1}{2}A_{1/2}(\tau), \\ F_{pf}(\tau) &= \frac{1}{2}A_{1/2}^A(\tau), \\ F_1(\tau) &= -A_1(\tau), \\ F_0(\tau) &= A_0(\tau), \end{aligned} \quad (\text{A17})$$

$$C_i = \lambda, \quad (\text{A18})$$

$$(c_\beta O_{2,i} + s_\beta O_{3,i}) = C, \quad (\text{A19})$$

and

$$\begin{aligned} g_{sf}^i &= -(\sqrt{2}G_\mu)^{1/2}m_f a = -\frac{g}{2M_W}m_f a, \\ g_{pf}^i &= -(\sqrt{2}G_\mu)^{1/2}m_f b = -\frac{g}{2M_W}m_f b. \end{aligned} \quad (\text{A20})$$